

## Article

# Remote State Design for Efficient Quantum Metrology with Separable and Non-Teleporting States

Rahul Raj <sup>1,†</sup> , Shreya Banerjee <sup>2,\*</sup>  and Prasanta K. Panigrahi <sup>2</sup><sup>1</sup> Physics Department, JECRC University, Jaipur 303905, Rajasthan, India; rahulrajalex@gmail.com<sup>2</sup> Department of Physical Sciences, Indian Institute of Science Education and Research Kolkata, Mohanpur 741246, West Bengal, India; pprasanta@iiserkol.ac.in

\* Correspondence: shreya93ban@gmail.com

† These authors contributed equally to this work.

**Abstract:** Measurements leading to the collapse of states and the non-local quantum correlations are the key to all applications of quantum mechanics as well as in the studies of quantum foundation. The former is crucial for quantum parameter estimation, which is greatly affected by the physical environment and the measurement scheme itself. Its quantification is necessary to find efficient measurement schemes and circumvent the non-desirable environmental effects. This has led to the intense investigation of quantum metrology, extending the Cramér–Rao bound to the quantum domain through quantum Fisher information. Among all quantum states, the separable ones have the least quantumness; being devoid of the fragile non-local correlations, the component states remain unaffected in local operations performed by any of the parties. Therefore, using these states for the remote design of quantum states with high quantum Fisher information can have diverse applications in quantum information processing; accurate parameter estimation being a prominent example, as the quantum information extraction solely depends on it. Here, we demonstrate that these separable states with the least quantumness can be made extremely useful in parameter estimation tasks, and further show even in the case of the shared channel inflicted with the amplitude damping noise and phase flip noise, there is a gain in Quantum Fisher information (QFI). We subsequently pointed out that the symmetric W states, incapable of perfectly teleporting an unknown quantum state, are highly effective for remotely designing quantum states with high quantum Fisher information.

**Keywords:** Quantum Fisher information; quantum metrology; parameter estimation; Werner states; quantum teleportation.



**Citation:** Raj, R.; Banerjee, S.; Panigrahi, P.K. Remote State Design for Efficient Quantum Metrology with Separable and Non-Teleporting States. *Quantum Rep.* **2021**, *3*, 228–241. <https://doi.org/10.3390/quantum3010013>

Academic Editor: Gregg Jaeger

Received: 31 December 2020

Accepted: 6 March 2021

Published: 9 March 2021

**Publisher's Note:** MDPI stays neutral with regard to jurisdictional claims in published maps and institutional affiliations.



**Copyright:** © 2021 by the authors. Licensee MDPI, Basel, Switzerland. This article is an open access article distributed under the terms and conditions of the Creative Commons Attribution (CC BY) license (<https://creativecommons.org/licenses/by/4.0/>).

## 1. Introduction

The precise measurement of a parameter is one of the most crucial tasks in scientific researches. The famous Cramér–Rao bound [1,2] provides a bound to the achievable precision of a parameter in terms of the statistical Fisher information [3–7]. It has been shown that the information of a quantum system can be expressed in terms of quantum Fisher information in measurement by considering all possible outcomes of the measurement [6]. Quantum metrology uses the entanglement of a quantum system to achieve better precision in the estimation of a parameter than achieved in the classical cases [8–12]. Quantum states that achieve and cross the maximal quantum Fisher information attained by the separable states representing the classical systems are considered to be metrologically useful [13–15]. In this work, we provide a protocol that can increase the quantum Fisher information of a separable state beyond the separable limit by using only local operations and classical communications (LOCC). The separable states possess the least quantum correlations, and the components of separable states are unaffected by the local operations performed on one of the states, therefore making them less prone to noises inflicted by the environment and easier to construct in a real quantum computer. Thus using them for remote design-

ing of quantum states with higher quantum Fisher information can have several feasible real-world applications in quantum information theory.

Quantum protocols like teleportation [16–19], and remote state preparation [20–24] make use of entangled states shared between two spatially separated parties such as a channel, and then perform LOCC to achieve their goal. In this work, we provide a quantum protocol, where two spatially separated parties, Alice and Bob, share an entangled quantum state as ‘channel’, and Alice prepares a state with higher quantum Fisher information at Bob’s end starting with an unknown 2-qubit single parameter Werner state [25]. We report that the average quantum Fisher information attained by Bob’s final states following the proposed protocol is found to be significantly higher than the quantum Fisher information obtained by Alice’s initial state for most values of the state parameter of the initial state. Our results state that for the separable initial states taken by Alice, the average QFI of Bob’s final state crosses the separable limit, making them useful in quantum metrology. We also show that the symmetric  $W$  state, known as unsuitable for perfect teleportation of an unknown quantum state [26,27], can effectively be used as a channel in this protocol to create a state with very high quantum Fisher information starting with a state which initially had very low QFI. We consider an example case where the shared channel is affected with an amplitude damping noise, and further show that even with a noisy state, gain in QFI can be achieved.

The paper is organized as follows: In Section 2 we discuss the importance of quantum Fisher information in parameter estimation tasks. We present our results in Section 3 along with the description of the protocol with examples. Section 4 discusses the achievements of the protocol in increasing quantum Fisher information of an unknown mixed state. We summarize our findings and conclude in Section 5 with future directions.

## 2. Quantum Fisher Information

Quantum Fisher information (QFI) holds a crucial role in the parameter-estimation theory as it provides a bound to the precision of estimating a parameter, i.e., the measurement sensitivity [28,29]. Following the famous Cramér–Rao bound in an unbiased estimation, the maximum achievable precision of a parameter  $\theta$  is limited by [1,2],

$$\delta\theta = \frac{1}{\sqrt{F_\theta}}, \quad (1)$$

where  $F_\theta$  is the quantum Fisher information of the parameter  $\theta$  [5,6]. In quantum metrology, to estimate a parameter  $\theta$ , one introduces  $\theta$  to an initial state  $\rho$  in the form of a phase-shift by applying a rotation operator  $U_\theta = \exp(i\theta J_{\hat{n}})$  on  $\rho$ , and obtaining  $\rho_\theta = U_\theta \rho U_\theta^\dagger$ , here  $J_{\hat{n}}$  is the collective spin operator in the  $\hat{n}$  direction [30,31]. The precise estimation of the parameter can then be calculated by measuring the quantum Fisher information  $F$  of the state  $\rho_\theta$  given as [12,31–34],

$$F = C_{max}, \quad (2)$$

where  $C_{max}$  is the largest eigenvalue of the matrix  $C_{kl}$  given by,

$$C_{kl} = \sum_{i \neq j} \frac{(\lambda_i - \lambda_j)^2}{\lambda_i + \lambda_j} [\langle i | J_k | j \rangle \langle j | J_l | i \rangle + \langle i | J_l | j \rangle \langle j | J_k | i \rangle]. \quad (3)$$

Here,  $\lambda_i$ ,  $\lambda_j$ , and  $|i\rangle$ , and  $|j\rangle$  are eigenvalues and eigenvectors of the state considered and,  $J_k$  and  $J_l$  are angular momentum along  $k$  and  $l$  direction.

The quantum Cramér–Rao bound (QCRB) is a widely accepted bound for quantum metrology that has been well explored in quantum estimation theory such as, to evaluate the bounds of the fidelity of the separation vector of the two incoherent point sources of unequal brightness [35]. Several propositions have been made to attain QCRB, and it has been shown in the estimation of an unknown phase that parameterizes an unknown

unitary with the optimal input state, QCRB is unattainable, although it can be achieved in the case of noisy channel estimations [36]. In this work, we have considered the quantum Fisher information related to a precise estimation of the parameter  $\theta$ , considering a rotation about only the  $x$  direction. In this case, one can measure the QFI attainable by the state  $\rho$  using [12],

$$F_x = 2 \sum_{i \neq j} \frac{(\lambda_i - \lambda_j)^2}{\lambda_i + \lambda_j} [\langle i | J_x | j \rangle \langle j | J_x | i \rangle], \quad (4)$$

where  $J_x$  is the angular momentum operator along the  $x$  direction.

In this work, we show that using a teleportation-like quantum communication protocol, one can increase the value of quantum Fisher information  $F_x$  attainable by an unknown 2-qubit Werner state [25] for most values of the state parameter. The description of the protocol and relevant results can be found in Section 3.

### 3. Protocol to Increase the QFI of an Unknown Mixed State

In several quantum communication tasks, two spatially separated parties, usually named Alice and Bob, share a quantum channel and try to achieve their goal by using local operations and classical communications. In our protocol, using a pure quantum state with more than two qubits as a channel, Alice tries to prepare an unknown two-qubit Werner state given as [25],

$$\rho_A = \lambda |\phi\rangle \langle \phi| + (1 - \lambda) \frac{\mathbb{I}}{4} \quad (5)$$

at Bob's end, where  $|\phi\rangle$  is the Bell state  $\frac{1}{\sqrt{2}}(|00\rangle + |11\rangle)$ ,  $\lambda \in [0, 1]$  is the state parameter of the Werner state, and  $\frac{\mathbb{I}}{4}$  is the maximally mixed state of dimension four. Using this protocol, we show that the quantum Fisher information state attained by the state prepared at Bob's end is greater than the state originally taken by Alice for most values of the state parameter  $\lambda$ .

In this protocol, Alice and Bob share an entangled quantum state with qubits more than two as the 'channel'. Exactly two qubits of this 'channel' are with Bob. Alice chooses a Werner state of the form  $\rho_A$ , as given in Equation (5), jointly measures the state along with her qubit(s) of the channel using a suitable basis of her choice, and communicates her measurement outcome to Bob over a classical channel. Depending on her outcome, Bob's state collapses to different states, and based on the classical information of Alice's outcome, Bob measures the QFI  $F_x$ , as given in Equation (4), of his state for individual outcomes. We show that for most values of the state parameter  $\lambda$  of the Werner state taken by Alice, the average Quantum Fisher information over all possible outcomes achieved by Bob's final state is greater than the quantum Fisher information obtained by Alice's original state. We provide a detailed description of the protocol in the form of an example, using the 4-qubit Greenberger–Horne–Zeilinger (GHZ) state as the channel.

#### 3.1. Increase of QFI Using 4-Qubit Channels

The 4-qubit GHZ state is given as,

$$|\Psi\rangle = \frac{1}{\sqrt{2}}(|0000\rangle + |1111\rangle) \quad (6)$$

Here, the first-two qubit of the GHZ state  $|\Psi\rangle$  belong to Alice and the last two belong to Bob. Alice selects an unknown mixed state of the form  $\rho_A$  creating a system of six qubits as,

$$\rho_s = \rho_A \otimes |\Psi\rangle \langle \Psi| \quad (7)$$

The first four qubits of the state  $\rho_s$  belongs to Alice, on which she performs a measurement using a basis of her choice. To depict the protocol, we select two completely

orthonormal bases of four qubit states, as given provided in Appendix A. Upon Alice's measurement, Bob's state collapses to,

$$\rho_B^i = \text{Tr}_{1234}[\hat{M}_i \rho_s \hat{M}_i^\dagger], \quad (8)$$

where,  $\{\hat{M}_i\}$  is the set of mathematical measurement operators, given as,  $\hat{M}_i = |b_i\rangle \langle b_i| \otimes \mathbb{I}$ ,  $|b_i\rangle$  is the  $i$ th state in the measurement basis  $B_1$ , and  $\mathbb{I}$  is the identity matrix of dimension 4 [24]. We calculate the quantum Fisher information of the state  $\rho_B^i$ . Since there are 16 outcomes possible for Alice's measurement, the state of Bob's qubits can collapse into 16 different  $\rho_B^i$ s. To address this issue, we have taken an equal average of the quantum Fisher information obtained by Bob's final states in our theoretical simulation, considering the equal occurrence of all possible outcomes of Alice's measurement.

Figure 1 depicts a comparison between the quantum Fisher information attainable by Alice's initial state  $\rho_A$  and the average over the quantum Fisher information obtained by Bob's final states as functions of the state parameter  $\lambda$  of the initial state chosen by Alice. As can be seen from Figure 1, the average QFI attained by Bob's states is greater than the same obtained by Alice's initial state for the values of the state parameter  $\lambda < 0.535$  (up to three decimal places), if Alice measures her qubit in basis  $B_1$ . If Alice uses  $B_2$  as her measurement basis, the average QFI obtained by final Bob's states is greater than the QFI of the initial state for the range of values of the initial state parameter  $\lambda = 0$  to  $\lambda = 0.42$  (up to three decimal places).

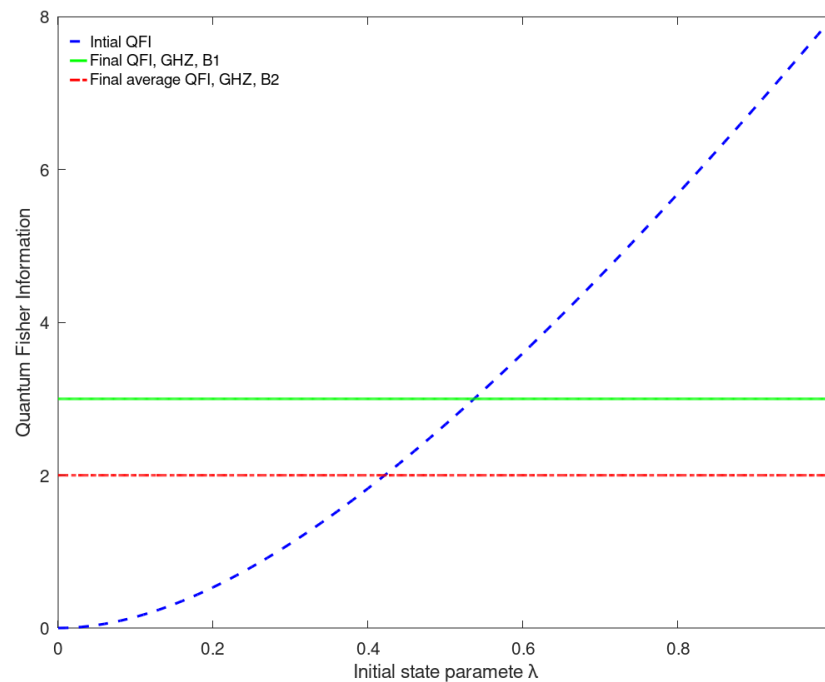


**Figure 1.** Comparison between the quantum Fisher information attainable by Alice's initial state  $\rho_A$  and the average over the quantum Fisher information obtained by Bob's final states, using 4-qubit Greenberger–Horne–Zeilinger (GHZ) state as a channel. The dashed blue line shows the variation of the quantum Fisher information as obtained by Alice's initial state with respect to the state parameter  $\lambda$ . The solid green line depicts the average quantum Fisher information obtained by Bob's final states as a function of the  $\lambda$  of the initial state, when Alice's register is measured in the basis  $B_1$ , and the red dashed-dotted line represents the final quantum Fisher information (QFI) obtained by Bob's state after Alice's qubits are measured in the basis  $B_2$ .

We have repeated the protocol using two other 4-qubit states as the channel shared by Alice and Bob; the 4-qubit cluster state used by Datta and Sarkar in [24], given as,

$$|\psi\rangle_C = \frac{1}{2}(|0000\rangle + |0110\rangle + |1001\rangle - |1111\rangle),$$

and the 4-qubit symmetric W state given by,

$$|\psi\rangle_W = \frac{1}{2}(|0001\rangle + |0010\rangle + |0100\rangle + |1000\rangle).$$

The comparison between the QFI attained by the initial state and the average over the final QFI using the states  $|\psi\rangle_C$ , and  $|\psi\rangle_W$  as channels is depicted in Figure 2.

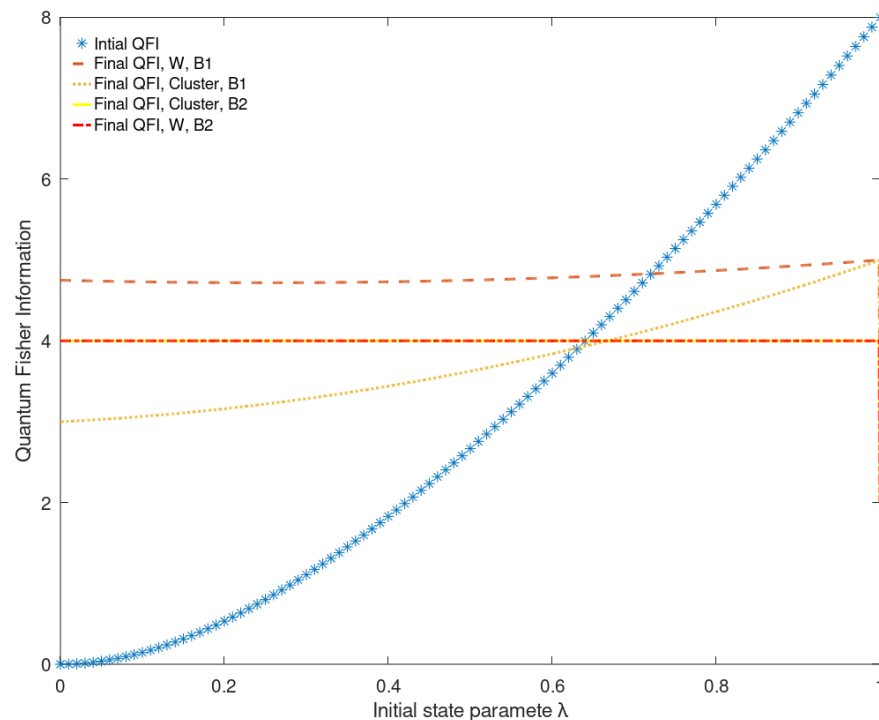


**Figure 2.** Comparison between the quantum Fisher information attainable by Alice’s initial state  $\rho_A$  and the average over the quantum Fisher information obtained by Bob’s final states, using the 4-qubit cluster state  $|\psi\rangle_C$ , and the 4-qubit symmetric W state as a channel. The blue line marked with ‘\*’s shows the variation of the quantum Fisher information as obtained by Alice’s initial state with respect to the state parameter  $\lambda$ . The dotted and solid yellow lines respectively depict the average quantum Fisher information obtained by Bob’s final states, when Alice measures her qubit in bases  $B_1$  and  $B_2$ , and the cluster state is used as a channel. The dashed and dashed-dotted red lines represent Bob’s average QFI, when the 4-qubit W state is used as a channel, and Alice’s register is measured in bases  $B_1$  and  $B_2$ , respectively.

Using the cluster state  $|\psi\rangle_C$  as the channel between the parties, the average value of quantum Fisher information attainable by Bob’s final states can be found to be greater than the QFI of Alice’s state for the range of the initial state parameter values  $[0, 0.632]$  and  $[0, 0.641]$  (approximated to three decimal places), when Alice’s qubits are measured in basis  $B_1$  and  $B_2$  respectively.

Similarly, if the 4-qubit symmetric W state is used as the channel, the average quantum Fisher information attainable by Bob’s final states is found to be greater than the QFI attained by Alice’s states to the state parameter values  $\lambda < 0.722$  and  $\lambda < 0.641$  (approximated to three decimal places) if Alice chooses to measure her register using basis  $B_1$  and  $B_2$ , respectively. It is worth mentioning here that it has been pointed out, the symmetric W state is unsuitable for perfect teleportation of an unknown state, as the non-local operations are required to retrieve the unknown state [26,27]. The aim of our protocol is to increase the quantum Fisher information achievable by the unknown state, not to retrieve the unknown

state. Here we show that although using only local operations and the symmetric W-state as a channel to teleport an unknown state is not possible, one can create a state with very high quantum Fisher information starting with a state that initially had very low QFI.

### 3.2. Increase of QFI Using 3-Qubit Channels

We have calculated the average final quantum Fisher information at Bob’s end using two different 3-qubit channels and two different measurement bases for Alice’s 3-qubit registers for each channel. We have used the 3-qubit GHZ state as well as the 3-qubit symmetric W state as channels, as provided in Equations (9) and (10). The measurement bases  $B'_1$  and  $B'_2$  are provided in Appendix B.

$$|\psi\rangle_{GHZ3} = \frac{1}{\sqrt{2}} |000\rangle + |111\rangle . \tag{9}$$

$$|\psi\rangle_{W3} = \frac{1}{\sqrt{3}} |001\rangle + |010\rangle + |100\rangle . \tag{10}$$

Figure 3 depicts the comparison between the QFI attained by the initial state and the average over the final QFI using the 3-qubit GHZ state and the symmetric 3-qubit W state as channels. As can be seen from Figure 3, the final average QFI of Bob’s states are higher than the QFI value of Alice’s initial state, up to state parameter values 0.639, and 0.641 when the 3-qubit GHZ state is used as a channel, and Alice uses bases  $B'_1$  and  $B'_2$  as her measurement bases, respectively. When the symmetric 3-qubit W state is used as the channel, the final average QFI attains a higher value than the initial QFI for  $\lambda < 0.546$  and  $\lambda < 0.828$ , respectively, for measurement bases  $B'_1$  and  $B'_2$  chosen by Alice.

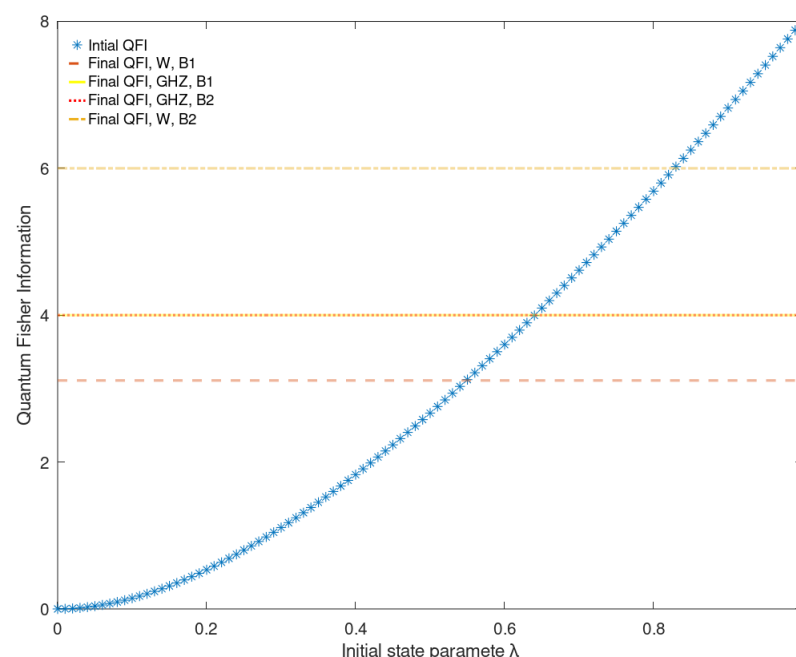


**Figure 3.** Comparison between the quantum Fisher information attainable by Alice’s initial state  $\rho_A$  and the average over the quantum Fisher information obtained by Bob’s final states, using 3-qubit GHZ state and 3-qubit W state as channels. The blue line marked with ‘\*’s shows the variation of the quantum Fisher information as obtained by Alice’s initial state with respect to the state parameter  $\lambda$ . The dotted and solid lines, respectively, depict the average quantum Fisher information obtained by Bob’s final states, when Alice measures her qubit in bases  $B'_1$  and  $B'_2$ , and the 3-qubit GHZ state is used as a channel. The dashed and dashed-dotted lines represent Bob’s average QFI, when the 3-qubit W state is used as a channel, and Alice’s register is measured in bases  $B'_1$  and  $B'_2$ , respectively.

#### 4. Discussion

Using a quantum communication protocol with an entangled channel of more than two qubits shared between two spatially separated parties Alice and Bob, we have shown that the quantum Fisher information (QFI) of an unknown mixed state can be increased using local operations and classical communications. It is noteworthy that for some of the measurement outcomes of Alice's register, the state prepared at Bob's end attains a QFI value eight for all values of the initial state parameter  $\lambda$ , the maximal QFI value attainable by the initial state for  $\lambda = 1$ , i.e., the QFI attainable by the Bell state; and for some measurement outcomes of Alice's states, the final state attains a much lesser QFI value. In Figure 4, we show an example of such a case, considering the 3-qubit W state as a channel, and  $B_2^1$  s Alice's measurement basis. As can be seen from Figure 4, the final QFI attained by Bob's state achieves value eight, when the outcome of Alice's state is  $|000\rangle$ ,  $|010\rangle$ ,  $|100\rangle$ , or  $|110\rangle$ . In case of Alice's outcome to be  $|000\rangle$ , and  $|010\rangle$ , the QFI attains value eight, for the entire range of the initial state parameter, while in case of Alice's outcome to be  $|100\rangle$ , and  $|110\rangle$ , the QFI drops at  $\lambda = 1$ . A similar case is observed if Alice measures her qubits to be in state  $|001\rangle$ ,  $|011\rangle$ ,  $|101\rangle$ , or  $|111\rangle$ . Here, in case of Alice's outcome to be  $|001\rangle$  or  $|011\rangle$ , the QFI attains a value of four for the entire range of the state parameter values, while drops at  $\lambda = 1$ , for Alice's outcomes being  $|101\rangle$  or  $|111\rangle$ . As is shown in Section 3 following this protocol and with a careful selection of channel and measurement basis for Alice, on average, the final states prepared at Bob's end can attain much higher quantum Fisher information than the initial states for a long-range of values of  $\lambda$ . Also, based on Alice's measurement outcomes, Bob can adjust his final state by means of local operations to achieve and ensure higher values of QFI for the entire range of the initial state parameter values.

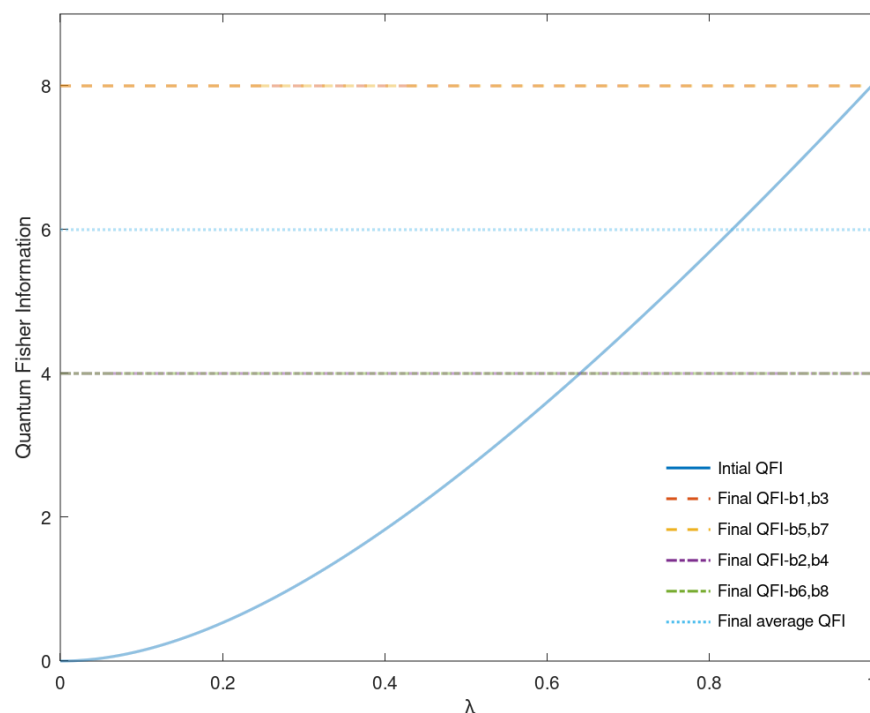


**Figure 4.** Final QFI attained by Bob's state for a different measurement outcome of Alice, with the 3-qubit W state as a channel and the computational basis ( $B_2^1$ ) as Alice's measurement basis. The solid blue line is the variation of QFI attained by Alice's state. The red and yellow dashed line (coincided at QFI = 8 for  $\lambda = [0, 1)$ ) represents Bob's QFI when Alice's registers as measured in states  $|000\rangle$ ,  $|010\rangle$ ,  $|100\rangle$ , or  $|110\rangle$ , and the violet and green dashed line (coincided at QFI = 4 for  $\lambda = [0, 1)$ ) represents Bob's QFI when Alice's registers as measured in states  $|001\rangle$ ,  $|011\rangle$ ,  $|101\rangle$ , or  $|111\rangle$ . The sky-blue dotted line represents the average QFI of Bob's final states.

As is well known, 2-qubit Werner states of form Equation (5) are separable for the range of state parameter values  $\lambda = [0, \frac{1}{3}]$  [25], i.e., the initial mixed state taken by Alice is separable for  $0 \leq \lambda \leq \frac{1}{3}$ . It has been shown that the maximal QFI achievable by an  $n$ -qubit separable state  $F_{sep}$  is bounded by  $F_{sep} \leq n$  [12,37]. Thus for the initial 2-qubit Werner state, for  $0 \leq \lambda \leq \frac{1}{3}$ , the maximal attainable QFI can never exceed  $F_x = 2$ . As can be seen from Section 3, in all the examples of our protocol, the final average QFI of Bob's states  $F_x$  is always  $\geq 2$ , the equality arising when the 4-qubit GHZ state is taken as the channel, and Alice measures her register in measurement basis  $B_2$ .

To discuss the generality of the protocol, we consider the general 3-qubit pure state as the shared channel between Alice and Bob. In this particular example, we have used the  $B'_2$  as Alice's measurement basis.

$$|\psi\rangle_{gen} = a_0 |000\rangle + a_1 |001\rangle + a_2 |010\rangle + a_3 |011\rangle + a_4 |100\rangle + a_5 |101\rangle + a_6 |110\rangle + a_7 |111\rangle. \tag{11}$$

As is clear from Figure 4, the QFI of Bob's final state depends on Alice's measurement outcomes, we investigate Bob's final states in each case of Alice's measurement outcome under the assumption that the state in Equation (11) is used as the channel between the two parties. We found that in the case that Alice's measurement outcome is  $|000\rangle, |010\rangle, |100\rangle, |110\rangle$ , the density matrix of Bob's state reads,

$$\rho_{Bob}^1 = \begin{pmatrix} \frac{a_0^2}{a_0^2+a_1^2+a_2^2+a_3^2} & \frac{a_0a_1}{a_0^2+a_1^2+a_2^2+a_3^2} & \frac{a_0a_2}{a_0^2+a_1^2+a_2^2+a_3^2} & \frac{a_0a_3}{a_0^2+a_1^2+a_2^2+a_3^2} \\ \frac{a_0a_1}{a_0^2+a_1^2+a_2^2+a_3^2} & \frac{a_1^2}{a_0^2+a_1^2+a_2^2+a_3^2} & \frac{a_1a_2}{a_0^2+a_1^2+a_2^2+a_3^2} & \frac{a_1a_3}{a_0^2+a_1^2+a_2^2+a_3^2} \\ \frac{a_0a_2}{a_0^2+a_1^2+a_2^2+a_3^2} & \frac{a_1a_2}{a_0^2+a_1^2+a_2^2+a_3^2} & \frac{a_2^2}{a_0^2+a_1^2+a_2^2+a_3^2} & \frac{a_2a_3}{a_0^2+a_1^2+a_2^2+a_3^2} \\ \frac{a_0a_3}{a_0^2+a_1^2+a_2^2+a_3^2} & \frac{a_1a_3}{a_0^2+a_1^2+a_2^2+a_3^2} & \frac{a_2a_3}{a_0^2+a_1^2+a_2^2+a_3^2} & \frac{a_3^2}{a_0^2+a_1^2+a_2^2+a_3^2} \end{pmatrix}.$$

Similarly, if Alice measures her three qubits in any of the states  $|001\rangle, |011\rangle, |101\rangle, |111\rangle$ , Bob's final state reads,

$$\rho_{Bob}^2 = \begin{pmatrix} \frac{a_4^2}{a_4^2+a_5^2+a_6^2+a_7^2} & \frac{a_4a_5}{a_4^2+a_5^2+a_6^2+a_7^2} & \frac{a_4a_6}{a_4^2+a_5^2+a_6^2+a_7^2} & \frac{a_4a_7}{a_4^2+a_5^2+a_6^2+a_7^2} \\ \frac{a_4a_5}{a_4^2+a_5^2+a_6^2+a_7^2} & \frac{a_5^2}{a_4^2+a_5^2+a_6^2+a_7^2} & \frac{a_5a_6}{a_4^2+a_5^2+a_6^2+a_7^2} & \frac{a_5a_7}{a_4^2+a_5^2+a_6^2+a_7^2} \\ \frac{a_4a_6}{a_4^2+a_5^2+a_6^2+a_7^2} & \frac{a_5a_6}{a_4^2+a_5^2+a_6^2+a_7^2} & \frac{a_6^2}{a_4^2+a_5^2+a_6^2+a_7^2} & \frac{a_6a_7}{a_4^2+a_5^2+a_6^2+a_7^2} \\ \frac{a_4a_7}{a_4^2+a_5^2+a_6^2+a_7^2} & \frac{a_5a_7}{a_4^2+a_5^2+a_6^2+a_7^2} & \frac{a_6a_7}{a_4^2+a_5^2+a_6^2+a_7^2} & \frac{a_7^2}{a_4^2+a_5^2+a_6^2+a_7^2} \end{pmatrix}.$$

To achieve a higher QFI value at his end, Bob needs to create a quantum state that provides the best QFI. From the expressions of  $\rho_{Bob}^1$  and  $\rho_{Bob}^2$ , it is easy to see that, for the teleportation incapable  $W$  states, Bob's final state takes the form of Bell states in the case Alice's measurement outcomes belong to the set consisting of  $|001\rangle, |011\rangle, |101\rangle, |111\rangle$ , and thus achieving the maximal QFI(8) for the entire range of the initial state parameter value. However, this is not the case in which the GHZ state is selected as the channel, and for this particular set of Alice's measurement basis, using the GHZ state as a channel, it can never achieve the maximal QFI. In the case that Alice and Bob use a 3-qubit state other than the GHZ and  $W$  state, they can choose the suitable co-efficient values for the state given in Equation (11) so that Bob's final state achieves the maximal value of QFI. The process also depends on the suitable choice of the measurement bases.

To comment on the limit number of qubits that can be entangled and used, the channel for the protocol that provides a gain in QFI over the input state of Alice, we present Figure 5. As can be seen from Figure 5, as the qubits in the channels increase, the gain in QFI decreases. We report that the trend shown in Figure 5 persists, and also, the resource cost increases as one increases the number of qubits in the entangled channel. Thus, for all practical purposes, the channel with the lowest number of qubits is the most suitable for our protocol.

This work shines a light on the usefulness of the symmetric  $W$  states to increase the quantum Fisher information of an unknown mixed state in a teleportation-like protocol,

although it is well known that symmetric  $W$  states are incapable of teleporting an unknown state [26,27]. As can be seen from Figure 3, when used as a channel between Alice and Bob, the symmetric 3-qubit  $W$  state provides a significant improvement in the average QFI of Bob's final states, compared to the QFI of the initially mixed state taken by Alice for the range of state parameter values when it is separable. The average QFI attained by Bob's final states is six, even with the separable initial states, which is much higher than the separable limit of two. Thus, this protocol provides a way to use separable state parameter estimation tasks, which can play a significant role in real-life noisy quantum computers, as separable states are less prone to decohering channel effects. As can be seen from Section 3, the final average QFI attains the same value for the entire range of the initial state parameter  $\lambda$  in some examples with the sole exception of  $\lambda = 1$ , i.e., where Alice tries to create the pure and maximally entangled Bell state at Bob's end. For  $\lambda = 1$ , the average value of QFI of the final state has a sudden drop. A similar phenomenon is also noticed in cases where the average quantum Fisher information does not have a constant value, but a gradual increase with the increase of  $\lambda$ . QFI, which quantifies the phase sensitivity of a quantum state, arises due to do phase transition, much like entanglement in a physical quantum system. The observation of a sudden drop in the quantum Fisher information in the final state while preparing a maximally entangled state may find a similarity with a phenomenon like an entanglement sudden death [38]. However, a simpler explanation can be, as at the value of the state parameter  $\lambda = 1$ , the Werner state is essentially the Bell state, a pure state, it only contains some of the states in the measurement bases of Alice, and probabilities of some of the outcomes are 0; whereas, for any other values of the state parameters, there is a finite probability of any of the measurement outcomes of Alice's states.

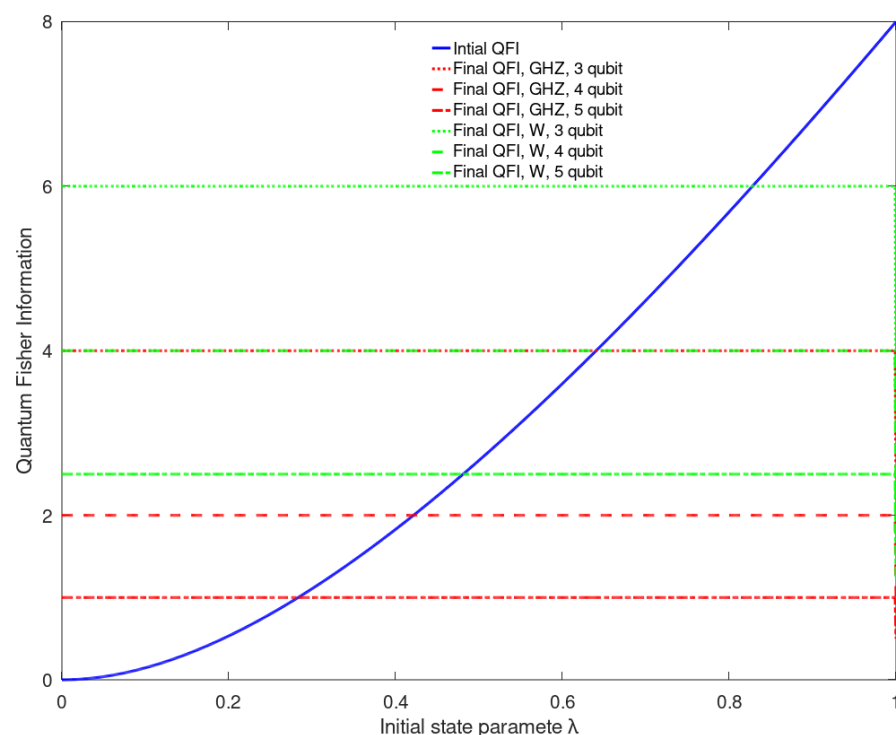


**Figure 5.** Average final QFI attained by Bob's state with the  $W$  and GHZ states as a channel with an increasing number of qubits and the computational basis ( $B_2'$ ) as Alice's measurement basis. The solid blue line is the variation of QFI attained by Alice's state. The green lines represent the QFI of Bob's state with  $W$  state as a channel, and the red lines represent the QFI of Bob's state with GHZ state as a channel.

To check how the protocol behaves in a real-world scenario, we have incorporated two simple noise models to the channel. In the first scenario, the amplitude-damping

noise inflicts all the channel qubits. In the second scenario, we consider a phase flip noise on all the channel qubits. The local Kraus operators for the amplitude damping channel (ADC) are,

$$K_1^i = |0\rangle\langle 0| + \sqrt{1-a}|1\rangle\langle 1|; K_2^i = \sqrt{a}|0\rangle\langle 1|,$$

and the phase flip noise are,

$$K_1^i = \sqrt{1-a}(|0\rangle\langle 0| + |1\rangle\langle 1|); K_2^i = \sqrt{a}(|0\rangle\langle 0| - |1\rangle\langle 1|),$$

where  $a$  is the noise parameter, and  $i$  is the local qubit on which the noise is applied.

Figure 6 depicts the average QFI of Bob's final states with respect to the noise parameter  $a$ , using a 4-qubit  $W$  state as a channel, inflicted with amplitude damping noise as well as phase flip noise, for a fixed value of the initial unknown state parameter  $\lambda = 0.25$ , well within the separable limit. In this case, Alice's register is measured in basis  $B_2$ . As is seen from Figure 6, the QFI of Bob's final state is greater than the QFI 0.8, obtained by Alice's initial state at a state parameter value of 0.25, for the entire range of the noise parameter value  $a$ , in both noise scenarios. So, while the gain in QFI obtained by Bob's final state through this protocol is found to be lowered in case the channel is inflicted with noise, but not diminished. We would like to mention, the increase of QFI with increasing noise in the system is similar to that of the GHZ states under amplitude damping noise, first demonstrated in [32]. Further such examples can be found in [39], in the case of bit-phase flip noise applied to the GHZ states. It will be interesting to see if the gain achieved by the presented protocol is retained by further complex noises, as an interesting line of further research.

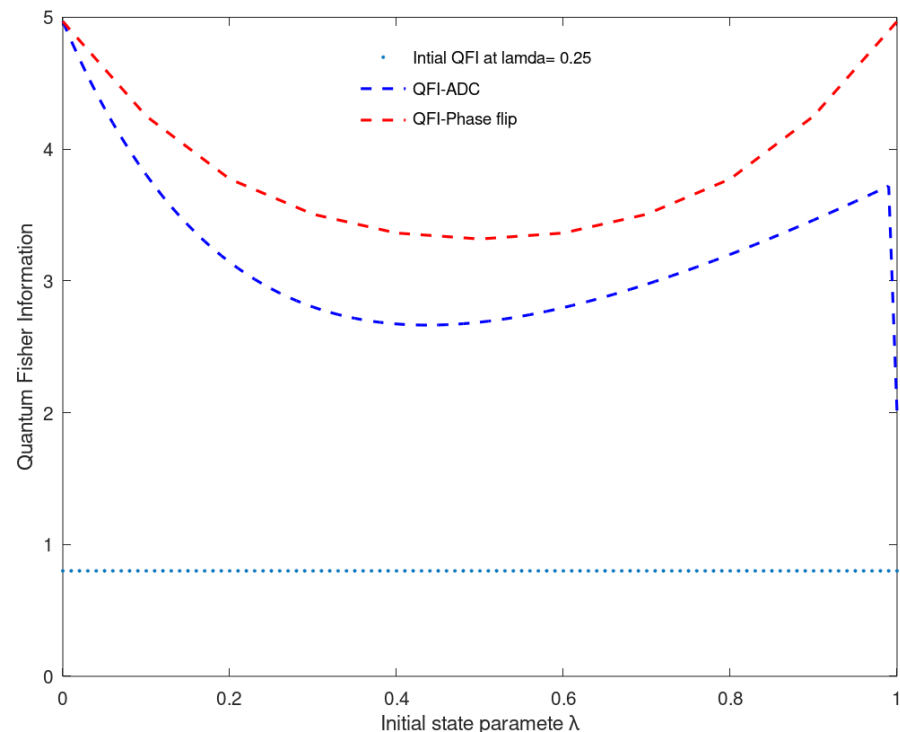


**Figure 6.** Average QFI attained by Bob's final states with respect to the noise parameter  $a$ , when the channel shared between the two parties taken as the 4-qubit  $W$  state is inflicted with amplitude damping noise (blue dashed line), and phase flip noise (red dashed line). In this example, the initial state parameter is taken to be 0.25, and Alice measures her register in basis  $B_2$ .

If one considers the noise induced in the initial unknown state taken by Alice, Werner states themselves can be seen as a pure maximally entangled state, with a possible noise introduced in them. As our protocol predicts the QFI attained by the final state prepared at Bob's end is constant for any values of the initial state parameter, there is an assured gain in the QFI of the state, in case the initial state is affected by noise.

Finally, we would like to enforce that, in our work, we have proposed a protocol to enhance the QFI of an unknown mixed state, by using the entangled resources. Although our protocol uses entangled states, they are only used to enhance the QFI of a different unknown mixed state, and not as a direct channel for metrology. This protocol is useful in a scenario where Alice and Bob are supposed to work with an unknown Werner state (unknown state parameter value), which can also be seen as a Bell state with possible (unknown) noise in the system in the two qubit scenario. Through our protocol, it is possible to enhance the QFI of the state with careful selection of the channel for a large range of values of the state (noise) parameters, as we have shown, the QFI attained by Bob's state is constant for any value of the state parameter. The increased QFI of the final state will help in better estimation of the parameter to be measured, as through the quantum Cramér–Rao bound, the uncertainty in the precision of measured precision is inversely proportional to the quantum Fisher information [1,2,36].

## 5. Conclusions

To summarize, we have shown in this work that with a shared entangled state between two spatially separated parties Alice and Bob, Alice can create a state at Bob's end that attains higher quantum Fisher information using only local operations and classical communication, starting with an initial unknown 2-qubit mixed state. Using five different 4 and 3-qubit entangled states as the shared channel between Alice and Bob, and two different measurement bases for each state, we have shown the value of the average final QFI depends on the channel and Alice's choice measurement bases, while it is independent of the initial state parameter. The average of the quantum Fisher information of the final Bob's states is taken over different measurement outcomes of Alice's register and is shown to attain a high value of QFI, which is above the separable limit for 2-qubit states for almost the entire range of the initial state parameter  $\lambda \in [0, 1)$  with a sudden drop at  $\lambda = 1$ , i.e., when Alice initiates the protocol with an entangled Bell state. The 2-qubit initial Werner states are separable in the limit of the parameter values  $0 \leq \lambda \leq \frac{1}{3}$ ; we have shown in this work, the final QFI attained by the state prepared at Bob's end is fairly higher than the separable limit when Alice's initial states are separable. This provides an advantage to the various real-world applications of quantum information theory that uses quantum Fisher information, as the separable states are easier to construct and less prone to noise, being devoid of the non-local correlations. Moreover, the symmetric W state, when taken as a channel in this teleportation-like protocol, is shown to provide betterment in the average final QFI over the QFI attained by the initial state, although this state is incapable of perfectly teleporting an unknown quantum state. It is observed that using the 3-qubit symmetric W state as a channel, for the range of the state parameter values  $\lambda \in [0, 0.828)$  (approximated to three decimal places), the final average QFI is higher than the initial state QFI if Alice chooses to measure her qubits in the computational basis. We have also shown that in the case in which the channel used by the parties is affected by an amplitude damping noise, the gain in the QFI by Bob's final state is not entirely diminished.

Quantum Fisher information plays a very significant role in parameter estimation tasks, as well as in quantum metrology. The states that attain a higher QFI value than the separable limit are said to be useful in metrology [12]; here we have provided a protocol to increase the quantum Fisher information of an unknown 2-qubit mixed state for most values of the state parameter  $\lambda$  beyond the separable limit. It has been shown that one can increase the QFI in entangled spin systems [40,41] by exciting the state of the system [31]. Here we show that using a simple protocol with LOCC, it is also possible to increase

the QFI of a quantum system beyond the separable limit, which can have significant practical applications.

Werner states are a class of  $n$ -qubit states that uses the similar form as in Equation (5), with  $n$ -qubit GHZ states as the maximally entangled states, and  $n$  qubit maximally mixed states [25]. The separable limit for such states is the state parameter  $\lambda = \frac{1}{n+1}$ . The measurement in Alice's register transfers the Werner state to an entangled state in Bob's register, and thus increasing the QFI of the unknown initial state. Such a protocol can easily be designed for a system with more than two qubits with correct selections of the channels shared between the parties and measurement basis chosen by Alice. The protocol is useful where Alice and Bob share an entangled resource, and an unknown channel is provided for the estimation of a parameter, such as in ion-trap quantum computers with distributed architectures. The observation of the gain in QFI where the shared entangled resource is inflicted with two important cases of noise shows that the protocol is useful in real life. However, further study is required in this direction to check the generality of the protocol, as well as its behavior in real quantum scenarios with several complex, noisy channels.

**Author Contributions:** R.R. and S.B. contributed equally to the development of the theoretical protocol, numerical simulations, and analysis of the results. S.B. conceived the project. P.K.P. supervised the research. All authors have read and agreed to the published version of the manuscript.

**Funding:** This research received no external funding.

**Institutional Review Board Statement:** Not applicable.

**Informed Consent Statement:** Not applicable.

**Acknowledgments:** S.B. acknowledges the Indian Institute of Science Education and Research Kolkata for partial supports. The authors thank the referees for careful reading and useful comments that helped to improve the paper.

**Conflicts of Interest:** The authors declare no competing interests.

## Appendix A

Measurement bases for Alice when she has a 4-qubit register:

**Measurement Basis  $B_1$ :**

$$\begin{aligned} |b_i\rangle &= (-1)^k (|\phi_{\pm}\rangle_{13} |00\rangle_{24} \pm |00\rangle_{13} |\phi_{\pm}\rangle_{24}); \\ |b_j\rangle &= (-1)^k (|\phi_{\pm}\rangle_{13} |11\rangle_{24} \pm |11\rangle_{13} |\phi_{\pm}\rangle_{24}); \\ |b_m\rangle &= (-1)^k (|00\rangle_{12} |\psi_{\pm}\rangle_{34} \pm |11\rangle_{12} |\phi_{\pm}\rangle_{34}); \\ |b_n\rangle &= (-1)^k (|01\rangle_{12} |\psi_{\pm}\rangle_{34} \pm |10\rangle_{12} |\phi_{\pm}\rangle_{34}); \end{aligned}$$

where,  $i \in \{1, 2, 3, 4\}$ ,  $j \in \{5, 6, 7, 8\}$ ,  $m \in \{9, 10, 11, 12\}$  and  $n \in \{13, 14, 15, 16\}$ ; and  $k = 1$  for  $i = 4, j = 8, m = 12$ , and  $n = 16$  otherwise,  $k = 0$ ; the numbers in the subscripts denote the qubit number in consideration.

$$|\psi_{\pm}\rangle = \frac{1}{\sqrt{2}} |00\rangle \pm |11\rangle;$$

and,

$$|\phi_{\pm}\rangle = \frac{1}{\sqrt{2}} |01\rangle \pm |10\rangle.$$

**Measurement Basis  $B_2$ :**

$$|b_i\rangle = |B_{i-1}\rangle,$$

where  $B_{i-1}$  is the decimal equivalent of the binary number  $i - 1$ , and  $i \in \{1, 2, 3, 4, 5, 6, 7, 8, 9, 10, 11, 12, 13, 14, 15, 16\}$ .

## Appendix B

Measurement bases for Alice when she has a 3-qubit register:

**Measurement Basis  $B'_1$ :**

$$|b_i\rangle = (-1)^k |\pm\rangle |\psi_{\pm}\rangle; |b_j\rangle = (-1)^k |\pm\rangle |\phi_{\pm}\rangle,$$

where,  $i \in \{1, 2, 3, 4\}$  and  $j \in \{5, 6, 7, 8\}$ ; and  $k = 1$  for  $i = 4$  and  $i = 8$ , otherwise,  $k = 0$ ;

$$|\pm\rangle = \frac{1}{\sqrt{2}} |0\rangle \pm |1\rangle;$$

$$|\psi_{\pm}\rangle = \frac{1}{\sqrt{2}} |00\rangle \pm |11\rangle;$$

and,

$$|\phi_{\pm}\rangle = \frac{1}{\sqrt{2}} |01\rangle \pm |10\rangle.$$

**Measurement Basis  $B'_2$ :**

$$|b_i\rangle = |B_{i-1}\rangle,$$

where  $B_{i-1}$  is the decimal equivalent of the binary number  $i - 1$ , and  $i \in \{1, 2, 3, 4, 5, 6, 7, 8\}$ .

## References

1. Cramér, H. *Mathematical Methods of Statistics*; Princeton University Press: Princeton, NJ, USA, 1946.
2. Radhakrishna Rao, C. Information and the accuracy attainable in the estimation of statistical parameters. *Bull. Calcutta Math. Soc.* **1945**, *37*, 81–91.
3. Fisher, R.A. Theory of Statistical Estimation. *Math. Proc. Camb. Philos. Soc.* **1925**, *22*, 700–725. [[CrossRef](#)]
4. Zegers, P. Fisher Information Properties. *Entropy* **2015**, *17*, 4918–4939. [[CrossRef](#)]
5. Ji, Z.; Wang, G.; Duan, R.; Feng, Y.; Ying, M. Parameter Estimation of Quantum Channels. *IEEE Trans. Inf. Theory* **2008**, *54*, 5172–5185. [[CrossRef](#)]
6. Braunstein, S.L.; Caves, C.M. Statistical distance and the geometry of quantum states. *Phys. Rev. Lett.* **1994**, *72*, 3439–3443. [[CrossRef](#)]
7. Mukherjee, N.; Majumdar, S.; Roy, A.K. Fisher information in confined hydrogen-like ions. *Chem. Phys. Lett.* **2018**, *691*, 449–455. [[CrossRef](#)]
8. Giovannetti, V.; Lloyd, S.; Maccone, L. Advances in quantum metrology. *Nat. Photonics* **2011**, *5*, 222–229. [[CrossRef](#)]
9. Tóth, G.; Apellaniz, I. Quantum metrology from a quantum information science perspective. *J. Phys. A Math. Theor.* **2014**, *47*, 424006. [[CrossRef](#)]
10. Panigrahi, P.; Kumar, A.; Roy, U.; Ghosh, S. Sub-Planck structures and Quantum Metrology. *AIP Conf. Proc.* **2011**, 1384. [[CrossRef](#)]
11. Yuan, H.; Fung, C.H.F. Quantum parameter estimation with general dynamics. *NPJ Quantum Inf.* **2017**, *3*, 14. [[CrossRef](#)]
12. Tóth, G.; Vértesi, T. Quantum States with a Positive Partial Transpose are Useful for Metrology. *Phys. Rev. Lett.* **2018**, *120*, 020506. [[CrossRef](#)] [[PubMed](#)]
13. Nielsen, M.A.; Chuang, I. *Quantum Computation and Quantum Information: 10th Anniversary Edition*; Cambridge University Press: Cambridge, UK, 2010.
14. Kalra, A.R.; Gupta, N.; Behera, B.K.; Prakash, S.; Panigrahi, P.K. Demonstration of the no-hiding theorem on the 5-Qubit IBM quantum computer in a category-theoretic framework. *Quantum Inf. Process.* **2019**, *18*, 170. [[CrossRef](#)]
15. Deutsch, J.M. Quantum statistical mechanics in a closed system. *Phys. Rev. A* **1991**, *43*, 2046–2049. [[CrossRef](#)]
16. Karlsson, A.; Bourennane, M. Quantum teleportation using three-particle entanglement. *Phys. Rev. A* **1998**, *58*, 4394–4400. [[CrossRef](#)]
17. Vaidman, L. Teleportation of quantum states. *Phys. Rev. A* **1994**, *49*, 1473–1476. [[CrossRef](#)]
18. El anouz, K.; El Allati, A.; Mourabit, T. Teleporting an unknown state using quantum Fisher information parameters. In Proceedings of the 2019 International Conference on Wireless Technologies, Embedded and Intelligent Systems (WITS), Fez, Morocco, 3–4 April 2019; pp. 1–5.
19. Paulson, K.G.; Panigrahi, P.K. Tripartite non-maximally-entangled mixed states as a resource for optimally controlled quantum teleportation fidelity. *Phys. Rev. A* **2019**, *100*, 052325. [[CrossRef](#)]
20. Pati, A.K. Minimum classical bit for remote preparation and measurement of a qubit. *Phys. Rev. A* **2000**, *63*, 014302. [[CrossRef](#)]
21. Kanjilal, S.; Khan, A.; Jebarathinam, C.; Home, D. Remote state preparation using correlations beyond discord. *Phys. Rev. A* **2018**, *98*, 062320. [[CrossRef](#)]
22. Dash, T.; Sk, R.; Panigrahi, P.K. Deterministic joint remote state preparation of arbitrary two-qubit state through noisy cluster-GHZ channel. *Opt. Commun.* **2020**, *464*, 125518. [[CrossRef](#)]

23. Barik, S.; Warke, A.; Behera, B.K.; Panigrahi, P.K. Deterministic hierarchical remote state preparation of a two-qubit entangled state using Brown et al. state in a noisy environment. *arXiv* **2020**, arXiv:2001.00574.
24. Sarkar, S.; Datta, C. Can quantum discord increase in a quantum communication task? *Quantum Inf. Process.* **2018**, *17*, 248. [[CrossRef](#)]
25. Banerjee, S.; Patel, A.A.; Panigrahi, P.K. Minimum distance of the boundary of the set of PPT states from the maximally mixed state using the geometry of the positive semidefinite cone. *Quantum Inf. Process.* **2019**, *18*, 296. [[CrossRef](#)]
26. Gorbachev, V.; Rodichkina, A.; Trubilko, A.; Zhiliba, A. On preparation of the entangled W-states from atomic ensembles. *Phys. Lett. A* **2003**, *310*, 339–343. [[CrossRef](#)]
27. Joo, J.; Park, Y.J.; Oh, S.; Kim, J. Quantum teleportation via aWstate. *New J. Phys.* **2003**, *5*, 136–136. [[CrossRef](#)]
28. Campbell, W.C.; Hamilton, P. Rotation sensing with trapped ions. *J. Phys. B At. Mol. Opt. Phys.* **2017**, *50*, 064002. [[CrossRef](#)]
29. Gilmore, K.A.; Bohnet, J.G.; Sawyer, B.C.; Britton, J.W.; Bollinger, J.J. Amplitude Sensing below the Zero-Point Fluctuations with a Two-Dimensional Trapped-Ion Mechanical Oscillator. *Phys. Rev. Lett.* **2017**, *118*, 263602. [[CrossRef](#)]
30. Hyllus, P.; Gühne, O.; Smerzi, A. Not all pure entangled states are useful for sub-shot-noise interferometry. *Phys. Rev. A* **2010**, *82*, 012337. [[CrossRef](#)]
31. Ozaydin, F.; Altintas, A.A. Quantum Metrology: Surpassing the shot-noise limit with Dzyaloshinskii-Moriya interaction. *Sci. Rep.* **2015**, *5*, 16360. [[CrossRef](#)]
32. Ma, J.; Huang, Y.X.; Wang, X.; Sun, C.P. Quantum Fisher information of the Greenberger-Horne-Zeilinger state in decoherence channels. *Phys. Rev. A* **2011**, *84*, 022302. [[CrossRef](#)]
33. Ozaydin, F. Quantum Fisher Information of a 3x 3 Bound Entangled State and its Relation with Geometric Discord. *Int. J. Theor. Phys.* **2015**, *54*, 3304–3310. [[CrossRef](#)]
34. Liu, J.; Yuan, H.; Lu, X.M.; Wang, X. Quantum Fisher information matrix and multiparameter estimation. *J. Phys. A Math. Theor.* **2019**, *53*, 023001. [[CrossRef](#)]
35. Prasad, S. Quantum limited super-resolution of an unequal-brightness source pair in three dimensions. *Phys. Scr.* **2020**, *95*, 054004. [[CrossRef](#)]
36. Hayashi, M.; Vinjanampathy, S.; Kwek, L.C. Resolving unattainable Cramér–Rao bounds for quantum sensors. *J. Phys. B At. Mol. Opt. Phys.* **2018**, *52*, 015503. [[CrossRef](#)]
37. Pezzé, L.; Smerzi, A. Entanglement, Nonlinear Dynamics, and the Heisenberg Limit. *Phys. Rev. Lett.* **2009**, *102*, 100401. [[CrossRef](#)] [[PubMed](#)]
38. Yu, T.; Eberly, J.H. Sudden Death of Entanglement. *Science* **2009**, *323*, 598–601. [[CrossRef](#)]
39. Falaye, B.J.; Adepoju, A.G.; Aliyu, A.S.; Melchor, M.M.; Liman, M.S.; Oluwadare, O.J.; González-Ramírez, M.D.; Oyewumi, K.J. Investigating quantum metrology in noisy channels. *Sci. Rep.* **2017**, *7*, 16622. [[CrossRef](#)] [[PubMed](#)]
40. Raj, R.; Sethi, S.; Behera, B.; Panigrahi, P. Quantum Simulation of Lattice Protein Models Using Quantum Annealing. 2020. Available online: <https://doi.org/10.13140/RG.2.2.34260.55687> (accessed on 16 April 2020).
41. Raj, R.; Kumar, M.; Behera, B.; Panigrahi, P. Simulation of Exchange Interaction and Entanglement Measure in Quantum Spin Systems. 2020. Available online: <https://doi.org/10.13140/RG.2.2.35538.91840> (accessed on 16 April 2020).